Doublet structure in the optical spectrum of a semiconductor laser with optoelectronic feedback in a square-wave regime

Md Shariful Islam, A. Kovalev, V. Iachkula, E. Viktorov, D. Citrin, A. Locquet

Doublet structure in the optical spectrum of a semiconductor laser with optoelectronic feedback in a square-wave regime

Md Shariful Islam,[1,2] A. V. Kovalev,[3] V. N. Iachkula,[3] E. A. Viktorov,[3] D. S. Citrin,[1,2] and A. Locquet[1,2]
[1)]*Georgia Tech-CNRS IRL 2958, Georgia Tech Lorraine, 2 Rue Marconi, 57070 Metz, France*
[2)]*School of Electrical and Computer Engineering, Georgia Institute of Technology, Atlanta,Georgia 30332-0250, USA*
[3)]*ITMO University, Birzhevaya Liniya 14, 199034 Saint Petersburg, Russia*

(*Electronic mail: alocquet@georgiatech-metz.fr)

(Dated: 7 December 2022)

We observe an optical spectrum consisting of a doublet in the output of a semiconductor laser diode with optoelectronic feedback in a dynamical regime in which a self-sustained square-wave modulation is observed, depending on injection current and feedback strength. The doublet frequency splitting is strongly correlated with the duty cycle of the square wave; both parameters, as well as the relative magnitude of the peaks, are observed to vary with the feedback level. A rate equation model reproduces the spectral doublets. The appearance of the doublet is attributed to active medium gain saturation and refractive index dependence on the carrier density.

A laser diode (LD) with optoelectronic (OE) feedback is known to exhibit a number of dynamical behaviors.[1] Amongst the most striking are periodic modulation of the optical output, including sinusoidal,[2] pulse trains,[3,4] and square waves (SW).[5–7] The rf spectrum (power spectrum of the optical intensity) directly reflects the dynamics of this modulation; however, less frequently is the *optical* spectrum characterized. This is because the optical phase information is lost at the photodetector in the feedback loop necessitating a phase-sensitive optical measurement. We have observed double-peaked optical spectra (doublet) when a LD is subjected to strong OE feedback with a saturable nonlinearity and produces square wave (SW) pulses, as reported recently.[6] When the injection current J is sufficiently above its threshold level J_{th}, SWs originate from a Hopf bifurcation scenario similar to that observed in gain-switched optical-pulse generation near J_{th}.[8] The SW repetition rate f_{rep} was found to be a harmonic of the feedback rate, *i.e.*, $f_{\mathrm{rep}} = n\tau^{-1}$. τ is the time delay of the OE feedback loop and n a small positive integer. The harmonic order n is found to increase with τ.[5] We have verified the presence of optical doublets for several n but present experimental results for representative cases.

Optical doublets have been previously observed in SWs produced by mode-locked fiber lasers.[9–12] The first theoretical report of optical SW generation from a fiber laser predicting optical doublets was presented in Ref. 13. In Ref. 14, stabilization of a single SW pulse in a fiber laser with anomalous dispersion leading to an optical doublet was studied numerically. It was found that the frequencies of the lines within the doublet remain the same, though the linewidth decreases with increasing J. The two frequencies result from the frequency shift due to the nonlinear refractive index variation of the anomalous dispersion fiber. Semaan *et al.* presented both experimental and numerical evidence of optical doublets in Ref. 11. In a dissipative soliton resonance region in a passively mode-locked fiber laser, a singlet-to-doublet transition with increasing J was found. The model accounting for this behavior includes gain saturation, dispersion in the refractive index, and nonlinearity in the losses.[11]

SW generation by a variety of semiconductor LDs has also been studied in recent years concentrating mostly on the generation mechanism and temporal dynamics.[7,15–19] SW dynamics in lasers with two polarization modes such as VCSEL, where the two intensity plateaus are related to polarization modes with different optical frequencies due to birefringence, is discussed in.[20,21] Otherwise, studies including optical spectra have been sparse.

In this Letter, we present experimental evidence of both singlet and doublet optical spectra in an edge emitting LD under OE feedback in a dynamical regime in which there is a SW component in the optical intensity output. The optical doublets in the current work are qualitatively comparable to double-peaked optical spectra of SWs in fiber lasers (*e.g.* Ref. 9–11) although the peaks in our report are separated by a few GHz, while the spacing in fiber lasers is on the order of a few THz. We observe a comb-like structure at f_{rep} frequency over the spectral peaks when the SW duty cycle is much smaller than 50%, a clear distinction with the spectra from fiber lasers where any secondary oscillation is absent for the optical doublets, perhaps because of the long fiber length. We account for the spectral splitting by a model incorporating nonlinear amplification and filtering present in the electronic path, the LD refractive index dependence on carrier density, and gain saturation.

The experimental setup is the same as in our recent work on the harmonic property of optical SWs.[5] An OE feedback is built around a multi-quantum well LD with $J_{th} = 20$ mA. A linear polarizer (LP) that transmits polarized beams depending on the position of its optical axis is mounted on a rotation stage to control the feedback level in the optical domain. The experimental feedback strength η is a relative measure of feedback level; it is determined by the angle between the LP axis and the direction of LD, $\eta = 1$ refers to full transmission and $\eta = 0$ refers to no transmission through the LP.[22] The band-pass electronic amplifiers used in the OE feedback loop have saturated output power rating of 23 dBm and are used to boost the photodetected signal before feeding it to the LD. For the measurement of the optical spectrum, the LD

output is split, half is used to measure the optical spectrum (Aragon Photonics, BOSA-200C spectrum analyzer) and the other half leads into the PD in the OE feedback loop and is used to monitor the optical intensity. The feedback is positive with $\tau = 33.64$ ns.

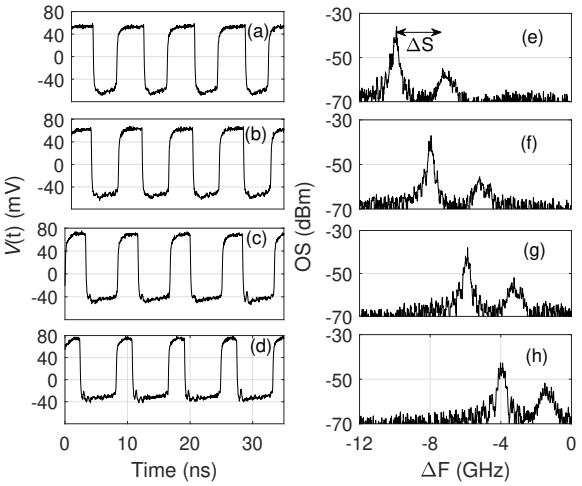

FIG. 1. PD output voltage $V(t)$ tracking the time-dependent AC component of optical intensity $I(t)$ (left-column) and corresponding optical spectra (right-column) where ΔF is the optical frequency measured from 194.083 THz corresponding to the output of the LD slightly above J_{th}. J is ramped down with $f_{\rm rep} = 4\tau^{-1}$ as (a) $J = 48.40$ mA, (b) $J = 43.00$ mA, (c) $J = 37.6$ mA, and (d) $J = 32.20$ mA. η is fixed at a moderately high value of 0.88. The SW duty cycle decreases with J but $f_{\rm rep}$ remains fixed; the splitting ΔS of the optical doublet decreases when J is ramped down.

As mentioned above, doublets are observed for all harmonic orders n for which SW generation occurs. For purposes of illustration, we show results for $n = 4$, *i.e.* $f_{\rm rep} = 4\tau^{-1}$. In Fig. 1, we start with fixed η and explore the square-waves (left-hand panel) with corresponding optical spectra (right-hand panel) as J is ramped down. In the left-hand panels, the PD voltage $V(t)$ is proportional to the AC component of the optical intensity $I(t)$. To observe the doublets presented in Fig. 1, we exploit the phenomena of hysteresis reported in Ref. 5 by stopping to ramp the current up at a J when LD pulsing turns into SWs and then ramping it down. The reason for ramping down is that at this J we are close to the operating limit of PD. By being in a lower J, we can access the SWs in a safe operating state of PD and explore the spectral dynamics. The following trends are observed when J is ramped down: the amplitude of the SW modulation remains nearly the same, the duty cycle (DC) decreases while the repetition rate $f_{\rm rep}$ remains constant, and the distance ΔS between the spectral peaks only slightly decreases. The shape of the spectral doublets remains practically unchanged but its location changes with the variation of J and shows current-dependent 0.5 GHz/mA spectral shift because of thermal effects, as expected.

In Fig. 2 we show the effect of varying η from 0.97 to 0.30 and holding J constant at 48.40 mA. The description of the left and right columns are same as in Fig. 1. Unlike the previous

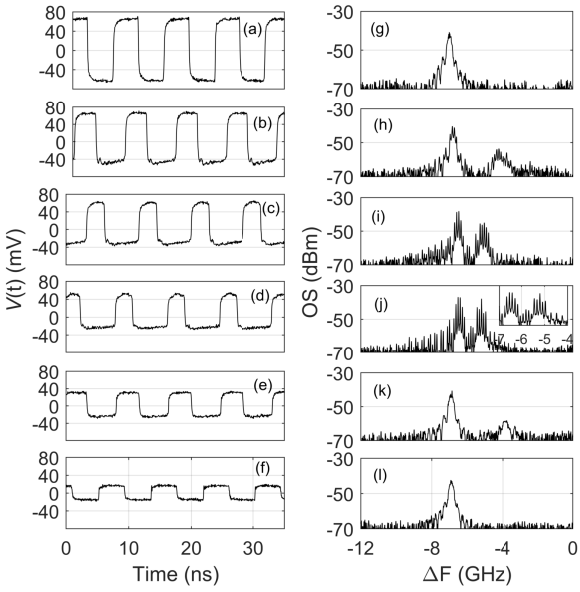

FIG. 2. PD output voltage $V(t)$ tracking the time-dependent AC component of optical intensity $I(t)$ (left-column) and corresponding optical spectra (right-column) for $J = 48.40$ mA as η is ramped down (a) 0.97, (b) 0.88, (c) 0.75, (d) 0.59, (e) 0.41, (f) 0.30 with $f_{\rm rep} = 4\tau^{-1}$. Note the appearance of doublets only for intermediate values of η with J held fixed. The inset in (j) shows evidence of the SW repetition rate $f_{\rm rep}$ in the spacing of the small peaks underlying the doublet. Note that the duty cycle is close to 50% in (a) and (l).

case where η was held fixed with J ramped down, here, with J held fixed and η ramped down, there is a decrease in the amplitude of the SWs. Another important difference is the non-monotonic evolution of DC and ΔS with the parameter variation.

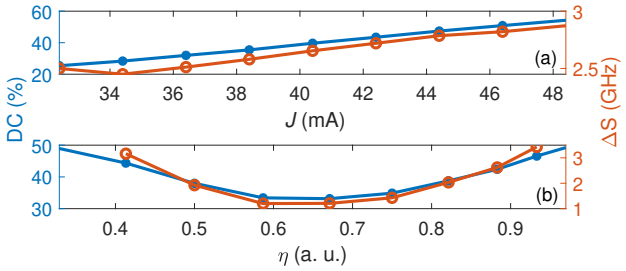

FIG. 3. On the right-hand scale, doublet splitting ΔS as functions of (a) J with $\eta = 0.88$ and (b) η with $J = 48.40$ mA. The left scale shows the duty cycle for comparison.

Figure 3 shows the dependence of DC and ΔS on J and η holding the other parameter fixed. DC appears to track ΔS. A perusal of Fig. 3 reveals that 20% to 60% variation of DC in Fig. 3(a) leads to a minor variation of ΔS, but 30% to 50% variation of DC in Fig. 3(b) leads to a much larger variation of ΔS. It suggests that DC and ΔS are not directly correlated but are linked by a common cause which still has to be identified. Specifically, the change with respect to η is almost parabolic

for both DC and ΔS, Fig. 3(b). It appears that varying η affects the amplifier saturation in a way that couples the changes in DC with the amplitude of the SWs. In our case, the carrier density is modulated in the SW regime thanks to gain saturation, modulating in turn the effective refractive index of the active medium and affecting the optical phase and spectrum. In particular, with the decrease in the amplitudes of the SW pulses in Figs. 2(a-d), the two peaks in the optical spectra become similar in magnitude and move closer to each other in Figs. 2(g-j). We have experimentally verified these trends for all other SW harmonics reported in Ref. 5.

To account for the observations discussed previously, we employ the single-mode semiconductor laser model described in Ref. 23 with the addition of nonlinear filtered feedback as in Ref. 5. The model describes the coupled nonlinear dynamics of the carrier density $N(t)$, the photon density $P(t)$, and the optical phase $\Phi(t)$. The model of the laser with feedback reads

$$\dot{N}(t) = \frac{I_{bias}+I_{fb}}{eV_{act}} - R(N) - \frac{\upsilon_g g(N)P(t)}{1+\varepsilon P(t)} + F_N(t), \quad (1)$$

$$\dot{P}(t) = \left[\frac{\Gamma\upsilon_g g(N)}{1+\varepsilon P(t)} - \frac{1}{\tau_p}\right] P(t) + \beta\Gamma BN^2(t) + F_P(t), \quad (2)$$

$$\dot{\Phi}(t) = \frac{\alpha}{2}\left[\Gamma\upsilon_g g(N) - \frac{1}{\tau_p}\right] + 2\pi\frac{df}{dT}\Delta T + F_\Phi(t), \quad (3)$$

$$\dot{I}_{FH,i}(t) = -{\tau_H}^{-1} I_{FH,i}(t) + \dot{I}_{FH,i-1}(t), \quad (4)$$

$$\dot{I}_{FL,j}(t) = -{\tau_L}^{-1}(I_{FL,j}(t) - I_{FL,j-1}(t)), \quad (5)$$

$$I_{fb} = s\tanh(k(I_{FL,M}(t-\tau) - \theta)), \quad (6)$$

where the dot means differentiation with respect to time t; I_{bias} is the injection current (corresponds to J in the experiment); I_{fb} is the feedback current, V_{act} is the volume of the active region; e is the electron charge; $R(N)$ is the carrier recombination rate; υ_g is the light group velocity in the active medium; $g(N)$ is the material gain; ε is the nonlinear gain coefficient; Γ is the optical confinement factor; τ_p is the cavity photon lifetime; β is the fraction of spontaneous emission coupled into the lasing mode; α is the linewidth enhancement factor; df/dT is the thermal variation of the emission frequency; ΔT is the difference between the active region temperature under the operating conditions and under the threshold current; $F_N(t)$, $F_P(t)$, and $F_\Phi(t)$ are Langevin noise terms; $I_{FH,i}(t)$ [$I_{FL,j}(t)$] is the filtered electric signal after the high- (low-) pass filter, $i = 1,\cdots,K$ ($j = 1,\cdots,M$) accounts for the K-th (M-th) order high- (low-) pass filtering [$I_{FH,0}(t) = \eta p_{out} P(t)$, $I_{FL,0}(t) = I_{FH,K}(t)$]; τ_H (τ_L) is the inverse of the cut-off frequency of the high- (low-) pass filter; η is the feedback strength; k is a small-signal amplification coefficient of the amplifiers; s is the maximum feedback current provided by an amplifier; θ is the amplification function asymmetry (offset) parameter, and p_{out} is the optical output power coefficient defined by

$$p_{out} = \frac{hf_0 V_{act}}{\Gamma\tau_p} \quad (7)$$

with h the Planck constant and f_0 the lasing frequency. (Refer to the supplementary material for details.)

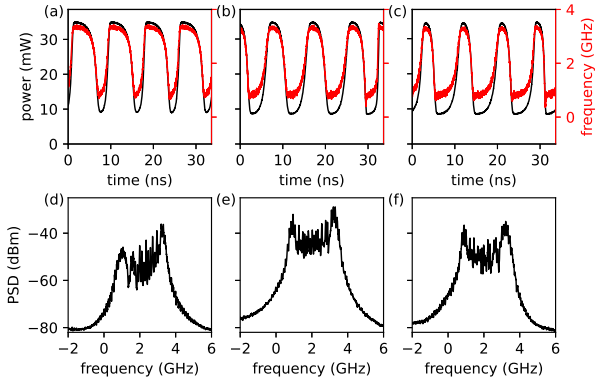

FIG. 4. Results obtained from Eqs. (1)–(6) with parameters in Table 1 in the Supplementary Material; the injection current $I_{bias} = 48.4$ mA, the feedback strength $\eta = 2.6\times10^{-3}$, and $\theta = -1.2$ μW (a, d), $\theta = 0$ μW (b, e), $\theta = 1.2$ μW (c, f). Black (red) curves in (a)–(c) show the optical power $p_{out}P(t)$ (instantaneous frequency $\dot{\Phi}(t)/(2\pi)$). The optical power spectral densities presented in (d)–(f) were obtained by Fourier transforming the complex electric field amplitude $\sqrt{p_{out}P(t)}\exp i\Phi(t)$ and subsequently filtering it with a Gaussian kernel of 10 MHz width to simulate the experimental spectrometer resolution.

The model parameters were partly deduced from the experimental relaxation oscillations, and partly taken from the literature, and are given in the supplementary material. Numerical simulations based on the model are shown in Fig. 4. For the parameters chosen, the model shows SW generation at the third harmonic of τ^{-1}, similar to what was reported in Ref. 5. Of note, the model also demonstrates the first and the second harmonics when η is varied.

Asymmetrical DC suggests an asymmetry in the nonlinear amplification which is modeled by a sigmoid function, Eq. (6). To model the asymmetry we introduce the θ parameter which shifts the sigmoid function towards a non-zero offset breaking the S-shaped symmetry of the amplification. The variation of θ provides a change in DC as illustrated in Fig. 4 for a set of θ values, which produce DC values of 67.4% (a), 50.1% (b), and 34.6% (c), but the amplitude of the SW and the doublet splitting remain practically unaffected in accordance with the results in Fig. 1. The θ acts in a way resembling the feedback offset phase responsible for the SW asymmetry in OE oscillators as reported in Refs. 24 and 25. We propose that θ is linearly dependent on J via the average signal power in the nonlinear feedback loop. The small experimental variation of ΔS in Fig. 3(a) can be related to the spectral shift of the doublet, as in Fig. 1, and the dispersion effect.

Unlike the variation of the pump current, the variation of the feedback strength does not result in a spectral shift of the low frequency peak in Fig. 2, whose location remains nearly fixed. The increase of η after the Hopf bifurcation[5] results in a larger amplitude of the SW and in a change of the SW profile: it is purely sine shaped at the Hopf bifurcation and becomes more flat-top shaped. We have checked that the change of the profile may have a strong effect on ΔS. The variation of DC in Fig. 3(b) with the feedback strength increase is, therefore, affected by at least three factors: the changing SW profile

(mostly at lower feedback strength), the change of the SW amplitude and the current in the nonlinear feedback, and the nonzero offset in the sigmoid function. The impact of the factors is different at different values of η, resulting in a curvilinear function in Fig. 3(b).

To specify the mechanism of the spectral doublet appearance, we analyze the SW generation. The SWs demonstrate two intensity plateaux that are defined by the maximum and minimum total injected current levels $(I_{bias}+s)$ and $(I_{bias}-s)$, respectively. The gain saturation, described by ε, leads to increase of the carrier density $N(t)$ with a photon density $P(t)$ increase, since more gain is needed to compensate the cavity losses. In turn, this variation in SW operation leads to two distinct lasing frequencies associated with plateaux through the change in the gain-medium refractive index characterized by the linewidth enhancement factor α. These frequencies form the two well-separated peak structure in the optical spectrum.

Neglecting thermal dynamics (*i.e.*, the dependence on ΔT and the corresponding frequency shifts on the total current injected) and taking $\Delta I = 2s$ as the injection-current difference for a SW operation, we obtain the difference between the plateaux optical frequencies $\Delta S = \Delta\omega_s/(2\pi) = 2.53$ GHz (see the supplementary material) which is close to ΔS in Fig. 4(d–f) and the experimentally observed values. The difference between this value and simulation results is related to a deviation of SW profile from an ideal flat-top oscillations.

In this work, we report an optical doublet in the output of a LD with nonlinear optoelectronic feedback operating in a square wave regime. This behavior has been observed for $f_{\text{rep}} = n\tau^{-1}$ for all n where square wave generation occurs. The duty cycle of the square wave appears to be strongly correlated to the frequency spacing of the doublets. A nonlinear model shows that the doublet originates in different laser frequencies in the high- and low-intensity states in the SW. This change in frequency is due to the gain saturation effect and the carrier-density dependence of the refractive index of the gain medium.

The observation of a doublet under SW operation may be of interest for compact photonic devices having applications in metrology, sensing, and mapping. The optical doublets produced by square waves presented here can be beneficial for hybrid AM/FM lidars since they provide both amplitude and frequency modulation that can be used for improving lidar performance by implementing multiple synchronized acquisition channels having just a single laser source.

SUPPLEMENTARY MATERIAL

The supplementary material contains the derivation of the spectral separation of an optical doublet and the list of model parameters used for the simulation.

AUTHOR'S CONTRIBUTIONS

All authors contributed equally to this work.

ACKNOWLEDGMENT

The work of A.V.K. and E.A.V. was supported by the Ministry of Education and Science of the Russian Federation (research project No. 2019-1442). E.A.V. was supported by the Professor@Lorraine grant from Lorraine Université d'Excellence. A.L., D.S.C., and M.S.I. acknowledge the financial support of the Conseil Régional Grand Est.

DATA AVAILABILITY

The data that support the findings of this study are available from the corresponding author upon reasonable request.

[1] Y. K. Chembo, D. Brunner, M. Jacquot, and L. Larger, "Optoelectronic oscillators with time-delayed feedback," Rev. Mod. Phys. **91**, 35006 (2019).
[2] M. J. Wishon, D. Choi, T. Niebur, N. Webster, Y. K. Chembo, E. A. Viktorov, D. S. Citrin, and A. Locquet, "Low-noise X-band Tunable Microwave Generator Based on a Semiconductor Laser with Feedback," IEEE Photon. Technol. Lett. **30**, 1597–1600 (2018).
[3] F. Lin and J. Liu, "Harmonic frequency locking in a semiconductor laser with delayed negative optoelectronic feedback," App. Phys. Lett. **81**, 3128–3130 (2002).
[4] F.-Y. Lin and J.-M. Liu, "Nonlinear dynamics of a semiconductor laser with delayed negative optoelectronic feedback," IEEE J. of Quantum Electron. **39**, 562–568 (2003).
[5] M. S. Islam, A. V. Kovalev, E. A. Viktorov, D. S. Citrin, and A. Locquet, "Optical square-wave generation in a semiconductor laser with optoelectronic feedback," Opt. Lett. **46**, 6031–6034 (2021).
[6] M. S. Islam, A. V. Kovalev, E. A. Viktorov, D. S. Citrin, and A. Locquet, "Optical square waves in a multiquantum-well laser with nonlinear optoelectronic feedback," in *Semiconductor Lasers and Laser Dynamics X*, Vol. 12141 (SPIE, 2022) p. 1214103.
[7] G. Friart, L. Weicker, J. Danckaert, and T. Erneux, "Relaxation and square-wave oscillations in a semiconductor laser with polarization rotated optical feedback," Opt. Express **22**, 6905 (2014).
[8] M. S. Islam, A. V. Kovalev, E. A. Viktorov, D. S. Citrin, and A. Locquet, "Microwave Frequency Comb Generation by Gain-Switching Versus Relaxation Oscillations," IEEE Photon. Technol. Lett. **33**, 491–494 (2021).
[9] X. Li, S. Zhang, H. Zhang, M. Han, F. Wen, and Z. Yang, "Highly Efficient Rectangular Pulse Emission in a Mode-Locked Fiber Laser," IEEE Photon. Technol. Lett. **26**, 2082–2085 (2014).
[10] X. Zhang, C. Gu, G. Chen, B. Sun, L. Xu, A. Wang, and H. Ming, "Square-wave pulse with ultra-wide tuning range in a passively mode-locked fiber laser," Opt. Lett. **37**, 1334 (2012).
[11] G. Semaan, A. Komarov, A. Niang, M. Salhi, and F. Sanchez, "Spectral dynamics of square pulses in passively mode-locked fiber lasers," Phys. Rev. A **97**, 2–6 (2018).
[12] G. Semaan, F. Ben Braham, M. Salhi, Y. Meng, F. Bahloul, and F. Sanchez, "Generation of high energy square-wave pulses in all anomalous dispersion Er:Yb passive mode locked fiber ring laser," Opt. Express **24**, 8399 (2016).
[13] P. Grelu, W. Chang, A. Ankiewicz, J. M. Soto-Crespo, and N. Akhmediev, "Dissipative soliton resonance as a guideline for high-energy pulse laser oscillators," J. Opt. Soc. Am. B **27**, 2336–2341 (2010).
[14] A. Komarov, A. Dmitriev, K. Komarov, D. Meshcheriakov, and F. Sanchez, "Spectral-doublet rectangular pulses in passive mode-locked fiber lasers with anomalous dispersion," Phys. Rev. A **94**, 1–5 (2016).
[15] M. Sciamanna, M. Virte, C. Masoller, and A. Gavrielides, "Hopf bifurcation to square-wave switching in mutually coupled semiconductor lasers," Phys. Rev. E **86**, 1–7 (2012).
[16] C. Masoller, M. Sciamanna, and A. Gavrielides, "Two-parameter study of square-wave switching dynamics in orthogonally delay-coupled semiconductor lasers," Philos. Trans. R. Soc. A **371** (2013), 10.1098/rsta.2012.0471.
[17] S.-S. Li, X.-Z. Li, J.-P. Zhuang, G. Mezosi, M. Sorel, and S.-C. Chan, "Square-wave oscillations in a semiconductor ring laser subject to counter-directional delayed mutual feedback," Opt. Lett. **41**, 812 (2016).

[18]M. Dillane, B. Tykalewicz, D. Goulding, B. Garbin, S. Barland, and B. Kelleher, "Square wave excitability in quantum dot lasers under optical injection," Opt. Lett. **44**, 347 (2019).

[19]J. Martínez-Llinàs, P. Colet, and T. Erneux, "Tuning the period of square-wave oscillations for delay-coupled optoelectronic systems," Phys. Rev. E **89**, 1–11 (2014).

[20]C.-H. Uy, L. Weicker, D. Rontani, and M. Sciamanna, "Sustained oscillations accompanying polarization switching in laser dynamics," Opt. Express **26**, 16917–16924 (2018).

[21]C.-H. Uy, L. Weicker, D. Rontani, and M. Sciamanna, "Optical chimera in light polarization," APL Photon. **4**, 056104 (2019).

[22]M. S. Islam, A. V. Kovalev, G. Coget, E. A. Viktorov, D. S. Citrin, and A. Locquet, "Staircase Dynamics of a Photonic Microwave Oscillator Based on a Laser Diode with Delayed Optoelectronic Feedback," Phys. Rev. Appl. **13**, 064038–1 (2020).

[23]A. Rosado, A. Perez-Serrano, J. M. G. Tijero, A. V. Gutierrez, L. Pesquera, and I. Esquivias, "Numerical and experimental analysis of optical frequency comb generation in gain-switched semiconductor lasers," IEEE Journal of Quantum Electronics **55**, 1–12 (2019).

[24]D. P. Rosin, K. E. Callan, D. J. Gauthier, and E. Schöll, "Pulse-train solutions and excitability in an optoelectronic oscillator," Europhysics Letters **96**, 34001 (2011).

[25]L. Weicker, T. Erneux, O. D'Huys, J. Danckaert, M. Jacquot, Y. Chembo, and L. Larger, "Strongly asymmetric square waves in a time-delayed system," Phys. Rev. E **86**, 055201 (2012).